AIP | Journal of Applied Physics

Electronic structure, surface morphology, and topologically protected surface states of Sb2Te3 thin films grown on Si(111)

L. Plucinski, A. Herdt, S. Fahrendorf, G. Bihlmayer, G. Mussler et al.

Citation: J. Appl. Phys. **113**, 053706 (2013); doi: 10.1063/1.4789353
View online: http://dx.doi.org/10.1063/1.4789353
View Table of Contents: http://jap.aip.org/resource/1/JAPIAU/v113/i5
Published by the American Institute of Physics.

JOURNAL OF APPLIED PHYSICS **113**, 053706 (2013)

Electronic structure, surface morphology, and topologically protected surface states of Sb_2Te_3 thin films grown on Si(111)

L. Plucinski,[1,2,3,a)] A. Herdt,[1,2] S. Fahrendorf,[1,3] G. Bihlmayer,[3,4] G. Mussler,[3,5] S. Döring,[2] J. Kampmeier,[3,5] F. Matthes,[1,3] D. E. Bürgler,[1,3] D. Grützmacher,[3,5] S. Blügel,[3,4] and C. M. Schneider[1,2,3]

[1]*Peter Grünberg Institut PGI-6, Forschungszentrum Jülich, D-52425 Jülich, Germany*
[2]*Fakultät für Physik and Center for Nanointegration Duisburg-Essen (CeNIDE), DE-47048 Duisburg, Germany*
[3]*Jülich Aachen Research Alliance-Fundamentals of Future Information Technologies (JARA-FIT), Jülich, Germany*
[4]*Peter Grünberg Institut PGI-1 and Institute for Advanced Simulation IAS-1, Forschungszentrum Jülich, D-52425 Jülich, Germany*
[5]*Peter Grünberg Institut PGI-9, Forschungszentrum Jülich, D-52425 Jülich, Germany*

(Received 21 December 2012; accepted 7 January 2013; published online 4 February 2013)

We have performed a combined spectroscopy and microscopy study on surfaces of $Sb_2Te_3/Si(111)$ thin films exposed to air and annealed under ultra-high vacuum conditions. Scanning tunneling microscopy images, with atomic resolution present in most areas of such processed surfaces, show a significant amount of impurities and defects. Scanning tunneling spectroscopy reveals the bulk band gap of ~170 meV centered ~65 meV above the Fermi level. This intrinsic *p*-type doping behavior is confirmed by high-resolution angle-resolved photoemission spectra, which show the dispersions of the lower Dirac cone and the spectral weight of the bulk valence bands crossing the Fermi level. Spin-polarized photoemission revealed up to ~15% *in-plane* spin polarization for photoelectrons related to the topologically protected Dirac cone states near the Fermi level, and up to ~40% for several states at higher binding energies. The results are interpreted using *ab initio* electronic structure simulations and confirm the robustness of the time-reversal symmetry protected topological surface states in Sb_2Te_3 in the presence of impurities and defects. © *2013 American Institute of Physics*. [http://dx.doi.org/10.1063/1.4789353]

I. INTRODUCTION

Topological insulators (TIs) are narrow band-gap semiconductors in which the bulk band character inversions, induced by spin-orbit interaction, lead to formation of gapless edge or surface states. These specific surface electronic properties are related to the prediction of the quantum spin Hall (QSH) effect,[1,2] where spin currents emerge at the edges of the material in the absence of any external magnetic field. First, experiments were performed on HgTe quantum wells,[3] which are two-dimensional TIs, for which the terms "QSH insulator" and "topological insulator" are synonymous. Soon angle-resolved photoemission spectroscopy (ARPES) experiments followed and the first three-dimensional (3D) TIs were discovered with $Bi_{1-x}Sb_x$ showing Dirac-type cones[4] similar to the ones found in graphene. Subsequent theoretical predictions suggested that Bi_2Te_3, Bi_2Se_3, and Sb_2Te_3, layered crystals comprising weakly bonded quintuple layers (QLs), have a potential in producing fully spin-polarized currents for spin-electronic applications,[5] and currently, the label "3D TIs" is mainly associated with these materials and their alloys.

Analytical models predict that the topological surface states (TSSs) are fully spin-polarized. In the bulk band structure near the Γ point, the band character order is inverted due to the spin-orbit interaction which, at the boundary of the crystal, leads to the formation of gapless edge-states that are protected by the time-reversal symmetry. A more accurate analysis of the TI states can be performed by using density functional theory (DFT), which predicts that in these tellurides and selenides TSSs are delocalized over the surface QL, their averaged spin polarization is below 100% due to spin-orbit entanglement,[6] and the vector of spin polarization changes its orientation between the subsequent atomic layers.[7,8]

Since the implementation into spintronic devices calls for thin film structures, it is mandatory to establish whether the relevant spin electronic properties of their surfaces can withstand the typical device processing conditions. In particular, it is important to determine whether the TSS with antisymmetric spin property $\boldsymbol{\sigma}(\boldsymbol{k}) = -\boldsymbol{\sigma}(-\boldsymbol{k})$ is present in the rough processed surfaces previously exposed to non-ultra-high vacuum (UHV) conditions.

Among the three parent 3D TI compounds, the attention of the photoemission studies has focused mainly on Bi_2Se_3 and Bi_2Te_3, since the Dirac cones states are occupied and can be easily probed for these compounds. In Bi_2Se_3 and Bi_2Te_3, the Dirac cone states could be observed after exposing cleaved surfaces to the atmospheric air,[9] and the robustness of the Dirac cone state was confirmed in Bi_2Te_3 thin films sputtered and annealed under UHV.[10] It was also shown that the Fermi level position within the gap can be

a)Electronic address: l.plucinski@fz-juelich.de.

adjusted by changing the x parameter in $(Bi_{1-x}Sb_x)_2Te_3$ ternary alloys.[11] Sb_2Te_3 has attracted relatively less interest with limited number of publications where the surface electronic structure was observed.[11–14] Therefore, it is important to characterize the spin electronic properties and the robustness of the Dirac cone state in the Sb_2Te_3 parent compound in the thin film form.

In this work, we have characterized the processed surfaces of Sb_2Te_3 films by scanning tunneling microscopy (STM) and scanning tunneling spectroscopy (STS) and probe the spin polarization of their surface electrons by spin-polarized ARPES (spinARPES). We determined the spin texture within the Fermi surface finding a maximum value for the spin polarization vector of ~15% in the *in-plane* direction (normal to the direction of propagation and the surface normal) with no observable *out-of-plane* component for the Dirac cone photoelectrons. The experimental results are interpreted by comparison to the local densities of states (LDOS) and the surface electronic band structure obtained from DFT calculations.

II. METHODS

The Sb_2Te_3 samples were grown by molecular beam epitaxy (MBE) on weakly n-type doped Si:P (111) substrates ($\rho = 3.6 - 5.5\,\Omega\,cm$), which were chemically cleaned by the RCA recipe[15] to remove contaminants and the native oxide. Prior to the deposition of the Sb_2Te_3 layer, the substrate was thermally treated at 700 °C for 20 min. The growth took place in a Te overpressure regime with a growth rate of 10 nm/h. The effusion cell temperatures were 450 °C and 315 °C for Sb and Te, respectively. The substrate temperature was kept at 550 °C throughout the growth. The single crystal structure of the film was characterized *ex-situ* by x-ray diffraction (XRD) and the thickness was determined from x-ray reflectivity (XRR) using a Bruker D8 XRD system in a symmetric $\theta/2\theta$ geometry.

The STM experiments have been carried out in a multichamber UHV system comprising a preparation chamber for sample cleaning and characterization and a STM operating at 5 K (Omicron LT-STM). STM tips were *ex-situ* electrochemically etched from a Cr rod in NaOH solution and *in-situ* flashed by electron-beam bombardment for several seconds to remove oxides. $I(V)$ spectra were recorded by modulating the bias voltage (2.7 kHz, 30 mV) and using lock-in detection.

For STM/STS and spin-polarized photoemission measurements, samples were cleaned by annealing under UHV at 250 °C for 2 to 5 min. For high resolution ARPES data shown here, samples were sputtered by 500 eV Ar ions and annealed at 250 °C for 5 min, however, virtually the same spectra could be obtained on annealed-only samples. Auger electron spectroscopy spectra (not shown here) revealed that the cleaning procedure removed surface oxides, whereas the carbon Auger feature was always present even in sputtered samples. The thickness of the annealed-only samples was ~16 nm, and sputtered and annealed samples was ~14 nm, determined from *ex-situ* XRR performed after the measurements. The high-resolution ARPES spectra were measured on samples kept at 15 K with an overall resolution of 10 meV at a laboratory based system using He I ($h\nu = 21.22$ eV) and Xe ($h\nu = 8.44$ eV) discharge sources[16] recently upgraded with a MBS A1 spectrometer. The spinARPES experiment has been carried out at Beamline 5 of the 1.5 GeV synchrotron radiation source DELTA (Dortmund, Germany) using linearly polarized light (photon energy $h\nu = 24$ eV) at an overall resolution of 150 meV.[17] The experimental end-station includes a commercial Scienta SES-2002 hemispherical spectrometer equipped with a combination of an optimized high transmission spin-polarized low-energy electron diffraction (SPLEED) based detector[18,19] and a two-dimensional delay-line-detector (DLD) system,[17] and allows to simultaneously measure one of the *in-plane* and the *out-of-plane* components of the spin polarization vector $\boldsymbol{P}$.

The theoretical simulations of electronic properties of the Sb_2Te_3 thin films system were performed using the DFT in the generalized gradient approximation[20] and full-potential linearized augmented plane wave (FLAPW) method implemented in the FLEUR code (for details, see Ref. 21) with spin-orbit coupling included in a non-perturbative manner.

III. RESULTS

A. Scanning tunneling spectroscopy

Atomically smooth terraces, as seen in previous studies,[12,13,22] could not be observed in STM images shown in Fig. 1, however, atomic resolution could be easily obtained in majority of the areas of the surface. We attribute the areas without atomic resolution to the high amount of surface impurities and defects, which compromise the feasibility of the STM measurement over larger lateral scales. We conclude that our cleaning process introduces surface defects and impurities, but it does not remove the large scale crystallinity.

Experimental and simulated STS spectra are presented in Fig. 2. The experimental spectrum in Fig. 2(a) suggests a bulk band gap of ~170 meV width centered approximately 65 meV above the Fermi level, which indicates the intrinsic p-type doping of the films, in agreement with previous studies.[13,22] It should be noted that the value of the fundamental gap in Sb_2Te_3 is not fully established with experimental values ranging between 150 and 300 meV,[23] and theoretical simulations disagree about the dispersion around Γ near the Fermi level.[5,13,24,25] The STS spectra are mainly sensitive to the density of states from k-vectors close to the center of the two-dimensional Brillouin-zone. Taking this into account,

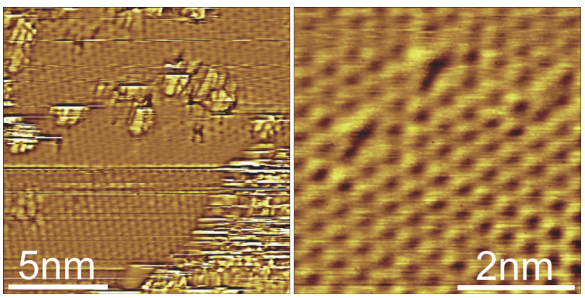

FIG. 1. Representative constant current STM images ($V = 1$ V, $I = 1$ nA) of the Sb_2Te_3 film. Atomic resolution is present in both images.

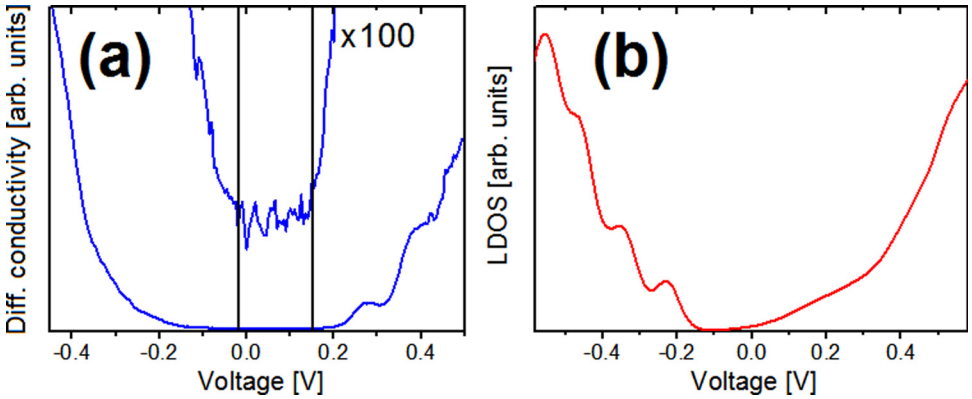

FIG. 2. (a) dI/dV spectra of the Sb_2Te_3 film recorded above areas with atomic resolution. $V_{stab} = 0.5$ V, $I_{stab} = 1$ nA, and $V_{mod} = 30$ mV. The magnified region shows the band gap of ~170meV. (b) Simulated LDOS of a 6QL Sb_2Te_3 film 3.7 Å above the surface.

the observed band gap width agrees reasonably with our DFT calculation and published data, however, this value contains no direct information on the size of an indirect bandgap, e.g., as predicted in Ref. 25.

The experimental STS spectrum also contains several features above the Fermi level, which were not observed for the surface of cleaved single crystal[13] and are not present in our simulated STS spectrum shown in Fig. 2(b). Recent high resolution STS results on *in-situ* grown thin films[22] indicate several shoulder-like features above the Fermi level related to the quantum wells along the surface normal for ultrathin films with thickness below 10 QL, however, our more pronounced features are originating from even thicker films. Therefore, we believe that the features above the Fermi level in our spectra are not due to quantum well states of clean Sb_2Te_3. It is known that cleaning methods under UHV may modify the bottom of the conduction band (CB) as shown for Bi_2Te_3 thin films[10] and introduce additional spectral weight in the local density of states along the surface normal. It is also known that a 2D electron gas develops on the surfaces of TIs as a result of the creation of extrinsic defects or the adsorption of impurities at the surface.[26] On the other hand, our STS measurements were performed on crystalline spots of the surface, which are free from visible impurities. Therefore, we conclude that the modification of conduction band spectral weight is related to modification of the ideal lattice by bulk impurities. Such processes can be simulated by assuming an expansion of the so-called van der Waals (vdW) gap between the QLs[27] which can be related to the intercalation of foreign atoms.[28]

The simulated STS spectrum reproduces the overall shape of the experimental spectrum, however, there are clear differences in fine structure. Clear modulations due to the quantum wells in the film with 6 QLs are predicted on the valence band (VB) side, consistent with previous STM results.[22,29] Our measured films with 16 QL were much thicker, and such modulations were not observed in the experimental data, which can be attributed to the narrower spacing of the quantum well states and the presence of defects. The slope of the CB is similar to the experimental one, however, without any clear features. The simulated spectrum contains spectral weight within the fundamental gap region, related to the Dirac cone states, which increases with the voltage. A similar effect can be observed in the experimental spectrum, however, there the ratio between the Dirac cone LDOS and the VB and CB LDOS is much smaller than predicted by the theory, possibly due to experimental tunneling conditions.

B. Spin- and angle resolved photoemission

Figure 3 shows high resolution ARPES results from a $Sb_2Te_3/Si(111)$ film kept at 15 K. Figure 3(a) presents the valence band spectrum measured using the He I ($h\nu = 21.22$ eV) radiation and dominated by the strongly dispersing bands between 0.5 and 5 eV binding energy. The most pronounced feature is the Rashba spin-split surface state between 0.5 and 1 eV binding energy. Figure 3(b) shows the electronic structure calculation for a 6 QL thick film with the spin-polarized (surface-related) features marked in color. There is an overall good agreement to the ARPES map shown in Fig. 3(a) suggesting that most of the features observed in ARPES are surface related. The highest spin polarization is expected for the Rashba state between 0.5 and 1 eV binding energy. Minor differences in band positions are typical for the DFT in particular far away from the Fermi level. Figures 3(c) and 3(d) present results at $h\nu = 8.44$ eV (Xe discharge). The Fermi surface of the circular shape and an intense spectral weight of six-fold symmetry, related to the valence band of Sb_2Te_3, is apparent in Fig. 3(c). Figure 3(d) clearly shows the lower Dirac cone state, along with the intense bulk bands, which reach to the Fermi level. The circular shape of the Dirac cone for various binding energies is also clear in Fig. 3(e), and from its dispersion slope in the region 100 meV below the E_F, we have found a Fermi velocity of $4.36 \cdot 10^5$ m/s (2.87 eV Å), which is higher than in single crystals.[13] The dispersion of the Dirac cone is nonlinear already in the region several tenths of meV away from the Dirac point, therefore, an accurate determination of the Dirac point position is not possible from the linear interpolation (which gives a Dirac point ~105meV above the Fermi level). A more accurate way is to match the experimental and the calculated band dispersions around the Fermi level, which we have performed in Fig. 3(f), and which resulted in the predicted Dirac point position of ~65 meV above the surface, a value consistent with the STS spectrum in Fig. 2(a).

A clear lower Dirac cone could not be observed in spectra measured at $h\nu = 21.22$ eV, and compared to the result from Fig. 3(a), the Rashba state is less pronounced at $h\nu = 8.44$ eV. In our interpretation, a large number of

surface impurities and defects move the TSS deeper inside the surface and produce a non-dispersive background spectral weight. Furthermore, lattice expansion due to the vdW intercalation can move the TSS electron density into the second QL.[27] Therefore, the spectral weight of the TSS is small, and it cannot be observed anymore in surface sensitive experiment at $h\nu = 21.22\,\text{eV}$ on top of the non-dispersive background spectral weight. Due to the increased bulk sensitivity at lower kinetic energies, the TSS can be observed at $h\nu = 8.44\,\text{eV}$, and the spectral weight of the bulk bands near the Fermi level increases, perhaps because the photoemission matrix elements at $h\nu = 8.44\,\text{eV}$ favor transitions from particular projected bulk bands.

We conclude that the combination of STS spectra and high-resolution ARPES maps shows the intrinsic *p*-type doping of the films, and suggests that the Fermi level is pinned at the valence band maximum of the Sb_2Te_3 bulk bands.

Spin-polarized photoemission measurements performed at 200 K at the rim of the Dirac cone for the two opposite symmetry directions are presented in Fig. 4. The polarization $P = A/S$ with the asymmetry $A = (I_L - I_R)/(I_L + I_R)$, in which I_L and I_R are the signals for the beams scattered from the W(001) crystal in opposite mirror directions, was computed using the Sherman function $S = 0.25$.[18,19] In analogy to the analysis shown in Ref. 30, the unpolarized constant background above E_F has been removed.

For the *in-plane* spectra, we have obtained P_x up to ~15% in the Dirac cone and in the wider energy range up to ~40% for the most pronounced β feature at $E_B \simeq 0.5\,\text{eV}$ related to the Rashba spin-split band (Figs. 3(a) and 3(b)). The same state has been recently observed in cleaved single crystal samples and analyzed in detail by Pauly *et al.*,[13] who have found that it resides within the spin-orbit gap and therefore is protected by symmetry according to the theory by Pendry and Gurman.[31] Furthermore, a number of additional spin polarized states were observed for higher binding energies, and all measured states are of helical nature, i.e., for all of them a spin reversal between the symmetric regions A and B is observed. The relative spin-polarization orientation agrees with the theoretical prediction (Fig. 3(b)), i.e., states α, ϵ, and the lower binding energy branch of the β Rashba state are oriented opposite to γ and δ. No significant polarization was observed in the *out-of-plane* spin component for any of the features.

Contrary to the initial theoretical predictions by Zhang *et al.*,[5] it has been shown by both theory and experiment[13,24]

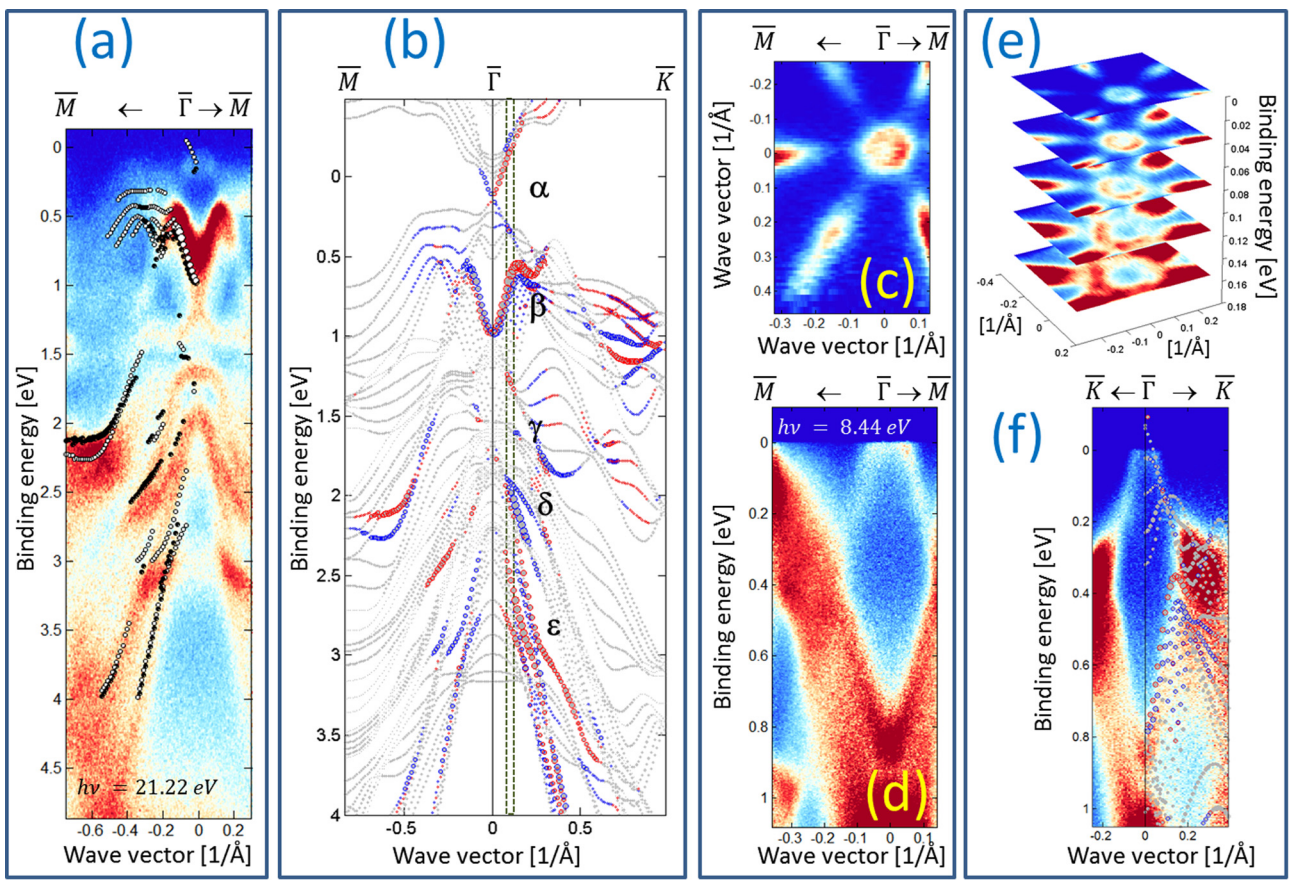

FIG. 3. Band structure of Sb_2Te_3 thin film. (a) ARPES map taken using He I ($h\nu = 21.22\,\text{eV}$) photons. (b) Calculated electronic structure of a 6 QL thick Sb_2Te_3 film along $\overline{\Gamma M}$ and $\overline{\Gamma K}$ directions. Red and blue symbols indicate states of opposite in-plane spin polarization vectors along the quantization axis perpendicular to the respective Brillouin zone trajectory. The size of the symbols is related to the spin polarization integrated over the distance z below the surface using the exponential decay $e^{-z/\lambda}$, where we assume $\lambda = 10$ Å for the photoelectron mean free path. In addition, the region related to the k-space integration of the spin-detector is shown, with the nomenclature of the most pronounced spectral features. States with significant in-plane spin polarization along $\overline{\Gamma M}$ are overlaid on top of the ARPES map in (a), here plotted with black and white symbols for better visibility. (c)-(f) Experimental results measured with Xe-discharge photons ($h\nu = 8.44\,\text{eV}$). (c) and (d) Fermi surface and ARPES map along $\overline{\Gamma M}$. (e) Stack of constant energy surfaces in the Dirac cone region and (f) ARPES map along $\overline{\Gamma K}$ with overlaid calculated bands shifted by 200 meV for the best fit in the Dirac cone region. Experimental results were measured on samples cooled down to 15 K and at a total experimental resolution of 10 meV.

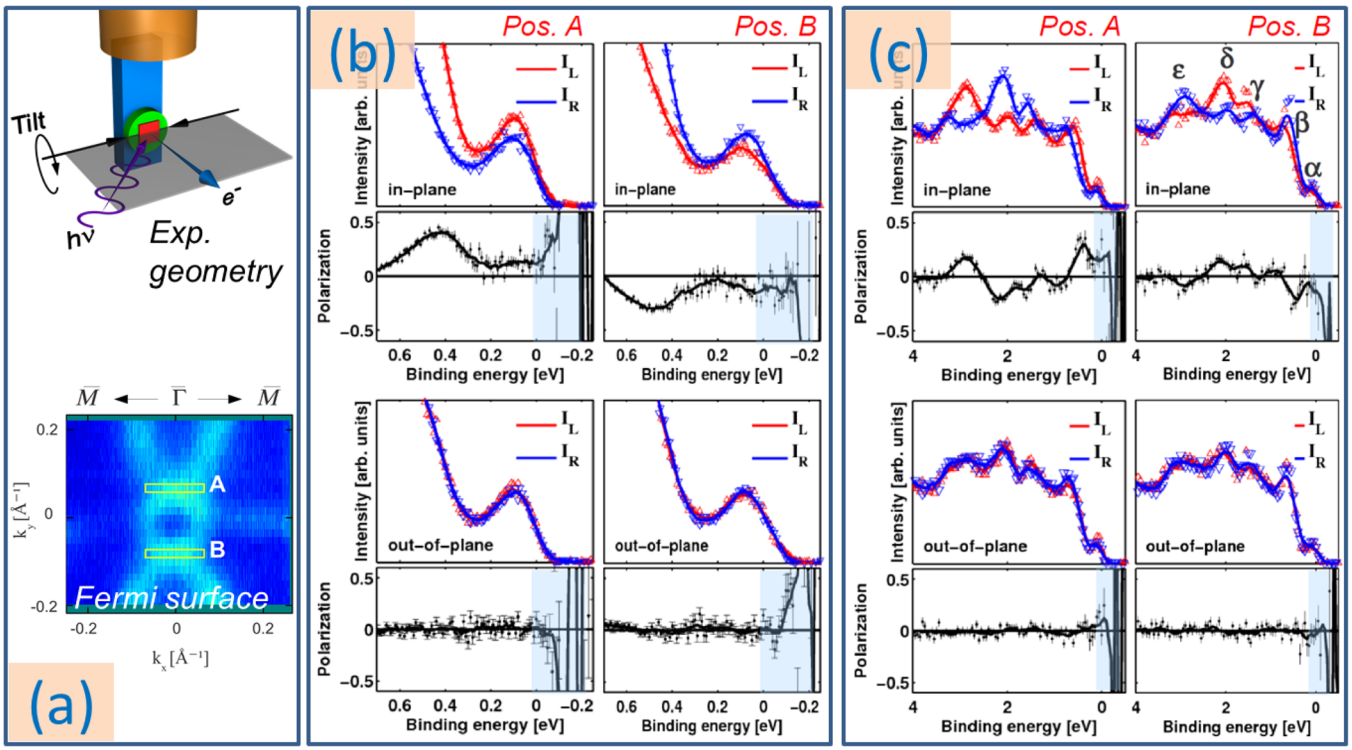

FIG. 4. Spin polarized spectra of a Sb_2Te_3 thin film. Experiments were performed at $h\nu = 24$ eV and 200 K with light linearly polarized in the horizontal plane and incident at 45°. (a) Fermi surface indicating the *k*-space positions A and B centered at $\pm 0.08 Å^{-1}$ which are integrated in the spin-resolved measurements.[17] These positions were set by adjusting the sample ("Tilt") as shown in the included schematic experimental geometry image. (b)-(c) SpinARPES spectra near the Fermi level and for the wider valence band range for the positions A and B.

that the separation of the Dirac point of Sb_2Te_3 from the projected bulk band structure is not pronounced. The lower Dirac cone of Sb_2Te_3 is almost an envelope for the projected bulk bands, a situation experimentally observed also in Bi_2Se_3.[32] A significant portion of unpolarized electrons, not only related to the surface impurities and defects but also to the projected bulk bands, might be mixed into the spectra, depending on the photoemission matrix elements for the particular photon energy. Furthermore, due to the spin-orbit entanglement, the effects related to symmetry in the photoemission experiment can influence the experimental spin polarization in the ensemble of photoemitted electrons.[33,34]

IV. SUMMARY

Our comprehensive study has combined microscopy and spectroscopy techniques to confirm the robustness of the time-reversal symmetry protected TSS in processed surfaces of Sb_2Te_3 thin films grown on Si(111). Exposure to atmospheric air and subsequent annealing under UHV resulted in a relatively rough surface covered by impurities and surface defects, however, on the majority of the surface area atomic resolution STM images could be obtained. STS spectra show the fundamental bulk gap of ~170 meV centered ~65 meV above the Fermi level. The overall shape of the experimental STS spectrum is in agreement with the one simulated for a 6 QL thick film, however, no modulation due to the quantum wells could be observed in the valence band side of the experimental spectrum, and the conduction band side of the experimental spectrum contains features which we assign to the modified bands in our processed films. These effects can be explained by impurities and intercalation in the vdW region. The lower Dirac cone state has been clearly observed in high-resolution ARPES band mapping at $h\nu = 8.44$ eV, and $E(k)$ and Fermi surface maps have confirmed the *p*-type character of the films, with the Fermi level pinned below the bulk VB maximum. SpinARPES measurements performed at $h\nu = 24$ eV confirmed the helical nature of the Dirac cone states with ~15% in-plane spin polarization in the ensemble of the photoemission electrons. Several other spin-polarized states of the helical nature have been identified in the wider range VB spinARPES spectra with spin polarization up to ~40% in agreement with the recent study on cleaved single crystals,[13] and the relative orientation of their spin-polarization vectors is in agreement with the theoretical prediction. Virtually no *out-of-plane* spin polarization component was observed in our study. Our study opens the path to use the properties of topologically protected states of such processed thin film surfaces for further investigations towards spintronic applications.

ACKNOWLEDGMENTS

We acknowledge the technical support of Bernd Küpper. This work was supported by a grant from the NRW Research School "Research with Synchrotron Radiation" funded by the Northrhine-Westphalia Ministry for Innovation, Science, Research, and Technology (Grant No. 321.2-8.03.06-58782).

[1]C. L. Kane and E. J. Mele, Phys. Rev. Lett. **95**, 146802 (2005).
[2]B. A. Bernevig and S.-C. Zhang, Phys. Rev. Lett. **96**, 106802 (2006).

[3]M. König, S. Wiedmann, C. Brüne, A. Roth, H. Buhmann, L. W. Molenkamp, X.-L. Qi, and S.-C. Zhang, Science **318**, 766 (2007).
[4]D. Hsieh, D. Qian, L. Wray, Y. Xia, Y. S. Hor, R. J. Cava, and M. Z. Hasan, Nature **452**, 970 (2008).
[5]H. Zhang, C. Liu, X. Qi, X. Dai, Z. Fang, and S. Zhang, Nat. Phys. **5**, 438 (2009).
[6]O. V. Yazyev, J. E. Moore, and S. G. Louie, Phys. Rev. Lett. **105**, 266806 (2010).
[7]S. V. Eremeev, G. Landolt, T. V. Menshchikova, B. Slomski, Y. M. Koroteev, Z. S. Aliev, M. B. Babanly, J. Henk, A. Ernst, L. Patthey *et al*., Nat. Commun. **3**, 635 (2012).
[8]J. Henk, A. Ernst, S. V. Eremeev, E. V. Chulkov, I. V. Maznichenko, and I. Mertig, Phys. Rev. Lett. **108**, 206801 (2012).
[9]C. Chen, S. He, H. Weng, W. Zhang, L. Zhao, H. Liu, X. Jia, D. Mou, S. Liu, J. He *et al*., Proc. Natl. Acad. Sci. U.S.A. **109**, 3694 (2012).
[10]L. Plucinski, G. Mussler, J. Krumrain, A. Herdt, S. Suga, D. Grützmacher, and C. M. Schneider, Appl. Phys. Lett. **98**, 222503 (2011).
[11]J. Zhang, C.-Z. Chang, Z. Zhang, J. Wen, X. Feng, K. Li, M. Liu, K. He, L. Wang, X. Chen *et al*., Nat. Commun. **2**, 574 (2011).
[12]G. Wang, X. Zhu, J. Wen, X. Chen, K. Z. Fang, J. Jia, and Q. Xue, Nano Res. **3**, 874 (2010).
[13]C. Pauly, G. Bihlmayer, M. Liebmann, M. Grob, A. Georgi, D. Subramaniam, M. R. Scholz, J. Sánchez-Barriga, A. Varykhalov, S. Blügel *et al*., Phys. Rev. B **86**, 235106 (2012).
[14]D. Hsieh, Y. Xia, D. Qian, L. Wray, F. Meier, J. H. Dil, J. Osterwalder, L. Patthey, A. V. Fedorov, H. Lin *et al*., Phys. Rev. Lett. **103**, 146401 (2009).
[15]J. Krumrain, G. Mussler, S. Borisova, T. Stoica, L. Plucinski, C. M. Schneider, and D. Gruetzmacher, J. Cryst. Growth **324**, 115 (2011).
[16]S. Suga, A. Sekiyama, G. Funabashi, J. Yamaguchi, M. Kimura, M. Tsujibayashi, T. Uyama, H. Sugiyama, Y. Tomida, G. Kuwahara *et al*., Rev. Sci. Instrum. **81**, 105111 (2010).
[17]L. Plucinski, A. Oelsner, F. Matthes, and C. M. Schneider, J. Electron Spectrosc. Relat. Phenom. **181**, 215 (2010).
[18]J. Kirschner and R. Feder, Phys. Rev. Lett. **42**, 1008 (1979).
[19]D. Yu, C. Math, M. Meier, M. Escher, G. Rangelov, and M. Donath, Surf. Sci. **601**, 5803 (2007).
[20]J. P. Perdew, K. Burke, and M. Ernzerhof, Phys. Rev. Lett. **77**, 3865 (1996).
[21]See http://www.flapw.de for a description of the code.
[22]Y. Jiang, Y. Y. Sun, M. Chen, Y. Wang, Z. Li, C. Song, K. He, L. Wang, X. Chen, Q.-K. Xue *et al*., Phys. Rev. Lett. **108**, 066809 (2012).
[23]*Landolt-Börnstein*, New Series Vol. 41C, edited by U. Rössler (Springer-Verlag, 1998), collaboration: Authors and editors of the volumes III/17E-17F-41C, http://www.springermaterials.com.
[24]S. Eremeev, Y. Koroteev, and E. Chulkov, JETP Lett. **91**, 387 (2010).
[25]T. Menshchikova, S. Eremeev, and E. Chulkov, JETP Lett. **94**, 106 (2011).
[26]M. Bianchi, D. Guan, S. Bao, J. Mi, B. B. Iversen, P. D. King, and P. Hofmann, Nat. Commun. **1**, 128 (2010).
[27]S. V. Eremeev, M. G. Vergniory, T. V. Menshchikova, A. A. Shaposhnikov, and E. V. Chulkov, New J. Phys. **14**, 113030 (2012).
[28]M. Ye, S. V. Eremeev, K. Kuroda, M. Nakatake, S. Kim, Y. Yamada, E. E. Krasovskii, E. V. Chulkov, M. Arita *et al*., e-print: arXiv:1112.5869v1.
[29]Y. Jiang, Y. Wang, M. Chen, Z. Li, C. Song, K. He, L. Wang, X. Chen, X. Ma, and Q.-K. Xue, Phys. Rev. Lett. **108**, 016401 (2012).
[30]C. Jozwiak, Y. L. Chen, A. V. Fedorov, J. G. Analytis, C. R. Rotundu, A. K. Schmid, J. D. Denlinger, Y.-D. Chuang, D.-H. Lee, I. R. Fisher *et al*., Phys. Rev. B **84**, 165113 (2011).
[31]J. Pendry and S. Gurman, Surf. Sci. **49**, 87 (1975).
[32]Y. L. Chen, J.-H. Chu, J. G. Analytis, Z. K. Liu, K. Igarashi, H.-H. Kuo, X. L. Qi, S. K. Mo, R. G. Moore, D. H. Lu *et al*., Science **329**, 659 (2010).
[33]C.-H. Park and S. G. Louie, Phys. Rev. Lett. **109**, 097601 (2012).
[34]J. Henk, A. Ernst, and P. Bruno, Phys. Rev. B **68**, 165416 (2003).